*36th EPS Conference on Plasma Phys. Sofia, June 29 - July 3, 2009 ECA Vol.**33E**, P-1.170 (2009)*

Spectroscopic diagnostics of the ablation clouds of injected pellets in LHD

M. Koubiti[1], M. Goto[2], S. Morita[2], R. Stamm[1]

[1]*PIIM UMR 6633 CNRS/Université de Provence, F-13397 Marseille Cedex 20, France*

[2]*National Institute for Fusion Science, Oroshi-cho 322-6, Toki 509-5292, Japan*

Abstract. Spectroscopic measurements related to intensities of spectral lines emitted by singly and doubly ionized aluminium ions are used for the determination of the main characteristics (electron density and temperature) of the ablation cloud of Al pellets injected in the Large Helical Device (LHD). Based on the assumption of Local Thermodynamic Equilibrium (LTE), this technique is successfully applied to obtain the temporal evolutions of ablation cloud plasma parameters over the period of the pellet ablation process.

1. Introduction

In devices dedicated to magnetically confined fusion plasmas, e.g., stellarators and tokamaks, pellet injection is seen as a major technique for deep plasma fuelling and plasma control by mitigating edge instabilities such as Edge Localized Modes (ELMs) or by triggering Internal Transport Barriers (ITBs) [1]. In several devices hydrogen/deuterium ice pellets are injected to extend the operational regime to higher densities which cannot be achieved by gas puffing while maintaining the dependence of the energy confinement on the density [2]. In LHD, pellets made of different materials are used. For instance carbon pellets are often injected for impurity transport studies [3-5] and in other cases aluminium and titanium pellets are used to obtain high-ion temperature plasmas. The injection process of a pellet can be characterized by two main parameters: the mass deposition profile and the penetration depth. From the early days of pellet injection, spectroscopy has played a key role in understanding the ablation process. In [5], the pellet penetration depth was measured and compared to predictions from the neutral gas model (NGS) and was linked to the pellet mass deposition profile. In this paper we present a spectroscopic study of the ablation cloud of pellets injected in the LHD.

2. Measurements

In LHD, pellets are injected thanks to a pneumatic pipe gun system which uses helium gas at a high pressure. Pellets are injected in the equatorial plane and travel the plasma with a speed estimated by the time-of-flight technique to ~200 m/s. Here we consider only aluminium pellets. Typically the later have cylindrical shapes with a length of 0.8 mm and a diameter of

0.5 mm. Their penetration depth is estimated to be ~1 m. A strong radiation in the visible spectral domain is emitted by the ablation cloud surrounding the pellet core. This radiation is collected using an optical fibre connected to a 0.5 m Czerny-Turner type spectrometer operating in the UV-visible. Spectra of this radiation are recorded using a CCD detector connected to the spectrometer with it entrance slit fixed at 50 μm. The major contribution to the observed spectra is due to lines emitted by singly and doubly ionized aluminium ions, i.e., Al^+ and Al^{2+}. The identified transitions used here are shown in Fig. 1.

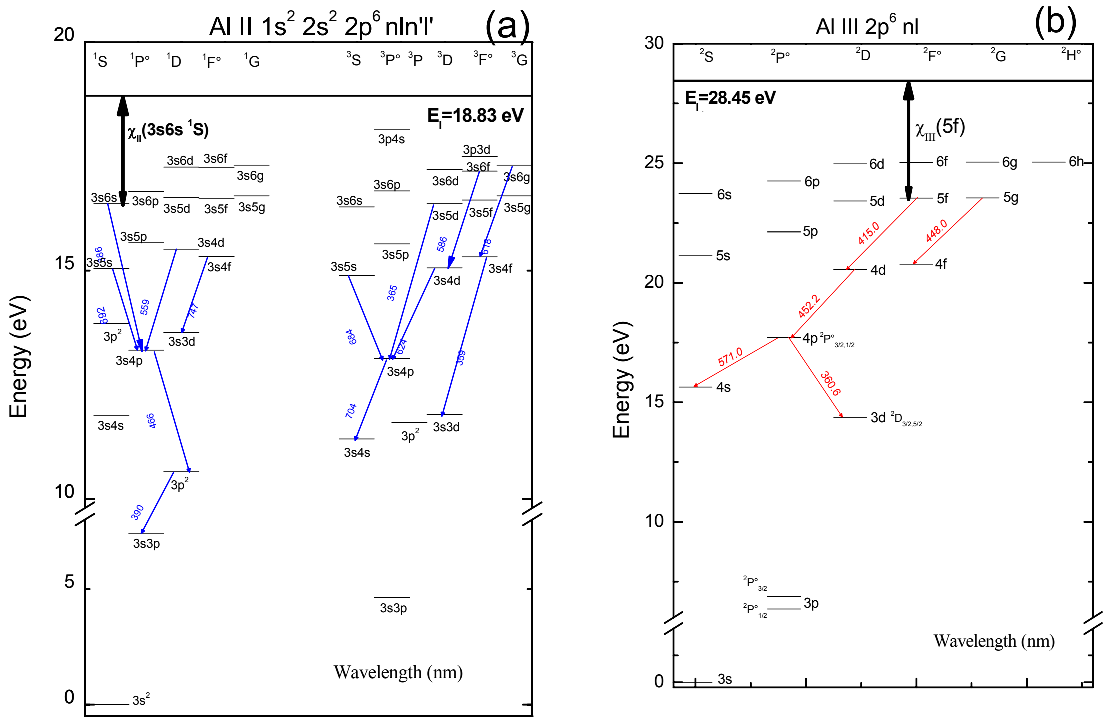

Fig. 1: Partial energy diagrams of Al^+ (a) and Al^{2+} (b) ions. Identified lines are shown by thin arrows. For both ions, ionization potentials from excited levels are shown by thick arrows while numerical values represent the ionization potential from the ground-states.

The intensities of the lines emitted by both ions are used to estimate the electron density (n_e) and temperature (T_e) of the plasma composing the ablation cloud of the pellet. It is assumed that Al^+ and Al^{2+} lines are emitted from the same cloud and that their level population densities are at LTE.

3. Theoretical background

The intensity I_{pq} of a line, i.e., a transition between an upper and lower levels p and q, emitted by a plasma having volume V is given by:

$$I_{pq} = h\nu \; n(p) \; A_{p\to q} \; V.$$

n(p) and $A_{p\to q}$ denote the population density of the upper level p and the transition probability. The volume-integrated population N(p)=n(p)V is obtained by dividing the intensity I_{pq} by $A_{p\to q}$ and the photon energy hν. The A-values are taken from NIST database [6] for almost all the lines, except for some few lines where refs. [7-9] were used. If an excited level p is in local thermodynamic equilibrium, then its population obeys the Saha-Boltzmann equation:

$$\frac{N_{III}(p)}{g_{III}(p)} = \frac{1}{2\,g_{IV}(1)}\left(\frac{h^2}{2\pi m k T_e}\right)^{3/2} \times \; e^{\left(\frac{\chi_{III}(p)}{k T_e}\right)} \times n_e N_{IV}(1) \qquad (1)$$

$N_{III}(p)$, $g_{III}(p)$, and $\chi_{III}(p)$ represent the population, statistical weight and ionization potential of level p of Al^{2+} ion and p=1 is the ground-state. Eq. (1) shows that, T_e is the parameter which governs the relative population distribution under LTE. Similarly under LTE assumption, the Al^{+} level populations, $N_{II}(p)$ obey to the following Saha-Boltzmann equation:

$$\frac{N_{II}(p)}{g_{II}(p)} = \frac{1}{2\,g_{III}(1)}\left(\frac{h^2}{2\pi m k T_e}\right)^{3/2} \times \; e^{\left(\frac{\chi_{II}(p)}{k T_e}\right)} \times n_e N_{III}(1) \qquad (2)$$

Furthermore under complete LTE, eq. (2) is valid for the ground state p=1 and one can write:

$$\frac{N_{II}(p)}{g_{II}(p)}\frac{2}{n_e}\left(\frac{h^2}{2\pi m k T_e}\right)^{-3/2} = \frac{1}{2\,g_{IV}(1)}\left(\frac{h^2}{2\pi m k T_e}\right)^{3/2} e^{\left(\frac{\chi_{III}(1)+\chi_{II}(p)}{k T_e}\right)} n_e N_{IV}(1) \qquad (3)$$

If the ionization potential for Al^{+} levels is measured from the ionization limit of Al^{2+}, then the right-hand side of eq. (3) becomes identical to that of eq. (1). To calculate the intensities, each identified spectral line is fitted with a Gaussian function with a FWHM ~1.5 nm representing the instrumental function. The experimental values of N(p)/g(p) for both Al^{+} and Al^{2+} ions, are shown in Fig. 2 using a logarithmic scale.

4. Results and discussion

From the visible spectroscopic measurements one estimates the duration of the ablation process of the aluminium pellets to be ~2-3ms. Most experimental population densities of Al^{+} and Al^{2+} ions agree with the corresponding LTE values even though deviations from LTE are observed for some few Al^{2+} levels. The electron temperature of the cloud surrounding the pellet core remains almost constant (~1.4 eV) along the ablation process as can be seen from fig. 2 (b). As the electron density of the pellet cloud is determined assuming a single emission zone for both Al^{+} and Al^{2+} ions and LTE for Al^{+} excited levels and all Al^{2+} levels including the ground state, the density values have to be crosschecked by comparison with other methods. One possibility is to use Stark broadening of emission lines to alternately determine the electron density of the pellet cloud. Such a technique will be applied to high-resolution spectra of Al^{+} and Al^{2+} VUV lines corresponding to transitions from high-n upper levels which may exhibit a significant Stark effect. The spectroscopic technique suggested here to characterize aluminium pellet ablation clouds will be extended to the case of titanium pellets often injected in LHD. A next step of this work is to check the consistency of the obtained results with those based on other methods, e.g., imaging spectroscopy and to link the cloud parameters to other quantities such as the deposition mass profile and the penetration depth.

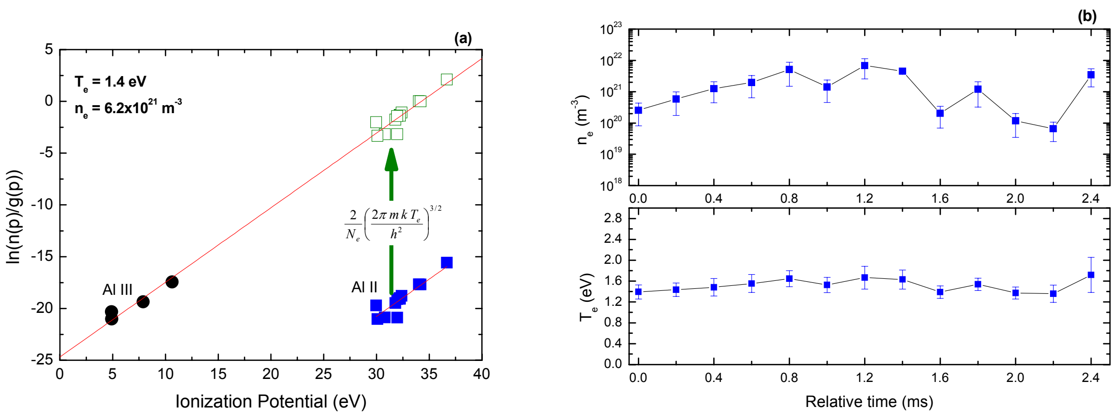

Fig. 2 Determination of the ablation cloud characteristics (n_e and T_e) from the fit of the experimental population densities of Al^{+} and Al^{2+} ions (a) and their temporal evolution over the ablation process duration of ~2-3 ms.

Acknowledgements

This work was supported by a NIFS invitation fellowship and the project "PHOTONITER" of the Agence Nationale de la Recherche (Contrat N° ANR-07-BLAN-0187-01).

References

[1] B. Pégourié, Plasma Phys. Control. Fusion **49**, R87 (2007).
[2] R. Sakamoto *et al*, Nucl. Fusion **44**, 624 (2004).
[3] H. Nozato *et al.*, Phys. Plasma **11**, 1920 (2004).
[4] H. Nozato *et al.*, Rev. Sci. Instrum. **76**, 073503 (2005).
[5] H. Nozato *et al.*, Phys. Plasmas **13**, 092502 (2006).
[6] Yu. Ralchenko *et al*, NIST Atomic Spectra Database (http://physics.nist.gov/asd3).
[7] Vujnoviæ *et al*, A&A 388, 704 (2002); T. Chang and R. Wang, Phys. Rev. A **36,** 3535 (1987).
[8] The atomic line list version 2.04 (Peter Van hoof): http://www.pa.uky.edu/~peter/atomic/.
[9] R. Payling and P. Larking, "Optical emission lines of the elements", ed. John Wiley & Sons (2000).